Scientific paper

Diaquabis(2,2'-dipyridylamine)M(II) Terephthalate Dihydrates, M(II) = Ni, Co: Synthesis, Crystal Structures, Thermal and Magnetic Properties

Lidija Radovanović,[1,*] Jelena Rogan,[2] Dejan Poleti,[2] Marko V. Rodić[3] and Zvonko Jagličić[4]

[1] *Innovation Centre - Faculty of Technology and Metallurgy, University of Belgrade, Karnegijeva 4, 11000 Belgrade, Serbia*

[2] *Department of General and Inorganic Chemistry, Faculty of Technology and Metallurgy, University of Belgrade, Karnegijeva 4, 11000 Belgrade, Serbia*

[3] *Faculty of Sciences, University of Novi Sad, Trg Dositeja Obradovića 3, 21000 Novi Sad, Serbia*

[4] *Faculty of Civil and Geodetic Engineering & Institute of Mathematics, Physics and Mechanics, University of Ljubljana, Jamova 2, 1000 Ljubljana, Slovenia*

** Corresponding author: E-mail: lradovanovic@tmf.bg.ac.rs phone: +381 11 3303784*

Received: 29-08-2017

Abstract

Two new isostructural M(II) (M = Ni, Co) complexes with 2,2'-dipyridylamine (dipya) and dianion of terephthalic acid (H_2tpht), [M(dipya)$_2$(H_2O)$_2$](tpht) · 2H_2O, have been synthesized by ligand exchange reaction and characterized by single-crystal X-ray diffraction, FTIR spectroscopy, TG/DSC analysis and magnetic measurements. The crystal structures of [M(dipya)$_2$(H_2O)$_2$](tpht) · 2H_2O consist of discrete complex units in which M(II) adopts deformed octahedral geometries. Two dipya ligands and two water molecules are coordinated to M(II) atom, tpht acts as a counter ion, while additional two water molecules remained uncoordinated. By numerous hydrogen bonds, all structural fragments are connected in three different chains which extend along [100], [010] and [001] directions, giving as a result a complex 3D network. The stabilization of 3D structure is accomplished by non-covalent face to face π-π interactions among pyridyl ring of dipya and benzene ring of tpht from adjacent chains. Towards the applied magnetic field, the both complexes exhibited almost perfect paramagnetic behavior.

Keywords: Co(II), Ni(II), 1,4-benzenedicarboxylate, discrete complex, magnetism

1. Introduction

The design and synthesis of mixed-ligand coordination compounds are of great significance in modern inorganic chemistry, which arise from their potential applications as functional materials and fascinating variety of topologies.[1] Concerning such topologies and functional properties, the essential step is to use the appropriate organic building units as well as metal ions. The anion of 1,4-benzenedicarboxylic (terephthalic, H_2tpht) acid, as one out of three positional isomers of benzenedicarboxylic (BDC) acids, is widely used as bridging ligand for designing new metal–organic compounds,[2,3] especially due to its diversity of the coordination modes, high structural stability, rigidity and planarity. Earlier studies[4,5] have vigorously stated that the usage of tpht ligand in combination with aromatic diamines as secondary ligands could afford a wide range of intriguing multi-dimensional structures with transition metal (TM) ions. The interest in tpht complexes is related to the molecular magnetism, and most published articles were focused on Cu(II) complexes and their magnetic properties together with an orbital interpretation of the magnetic exchange mechanism.[5–9]

2,2'-Dipyridylamine (dipya) as aromatic diamine ligand was not frequently used in combination with tpht. The survey of CSD showed[10] that only seven dipya–tpht complexes with different TM ions as nodes are structurally

characterized: $[Mn(dipya)_2(tpht)]_n$,[11] $[Mn(dipya)(H_2O)_4](tpht)$,[11] $[M(dipya)(tpht)(H_2O)_2] \cdot H_2O$ (M = Co, Ni),[12] $[Cu(dipya)(tpht)]_n$,[13] $\{[Cu_2(dipya)_2(tpht)_2] \cdot 2H_2O\}_n$[14] and $\{[Zn(dipya)(tpht)] \cdot H_2O\}_n$.[15] All Cu(II) compounds, $[Mn(dipya)_2(tpht)]_n$ and $\{[Zn(dipya)(tpht)] \cdot H_2O\}_n$ complexes take the form of zigzag chains, with tpht ligand acting in the range from bis-monodentate to bis-chelate bridge. On the other hand, Co(II) and Ni(II) compounds consist of discrete complex units, with tpht coordinated with only one COO group in a chelate mode, while another COO group remained uncoordinated. Only in $[Mn(dipya)(H_2O)_4](tpht)$, tpht was a counter anion. The role of tpht as counter anion as well as the hydrogen bond acceptor is not uncommon and it was described earlier for some TM–tpht complexes.[16–21] As a continuation of our ongoing studies on ternary TM complexes with tpht ions and some aromatic diamines, we present here the synthesis, crystal structure, thermal and magnetic properties of two new coordination compounds, with general formula $[M(dipya)_2(H_2O)_2](tpht) \cdot 2H_2O$, where M(II) = Ni, Co.

2. Experimental

2. 1. Materials and Measurements

Beside dipya and 1,10-phenanthroline (phen) which were of purum quality, all reagents were of analytical grade and used without further purification. $Ni(NO_3)_2 \cdot 6H_2O$, $Co(NO_3)_2 \cdot 6H_2O$ and phen were purchased from Merck (Germany). $Mn(NO_3)_2 \cdot 6H_2O$ was supplied by Carlo Erba (Italia), while dipya and EtOH were supplied by Sigma-Aldrich (USA). NaOH and H_2tpht were purchased by Alkaloid (Macedonia) and Ventron (United Kingdom), respectively.

FTIR spectra were recorded on a Bomem MB-100, Hartmann Braun FTIR spectrophotometer (4000–400 cm^{-1} region) using KBr pellets. Thermal properties of the complexes were examined from room temperature up to 1100 °C on an SDT Q600 TGA/DSC instrument (TA Instruments). The heating rate was 10 °C min^{-1} using less than 10 mg sample mass. The furnace atmosphere consisted of dry nitrogen at a flow rate of 100 cm^3 min^{-1}. X-ray powder diffraction (XRPD) data were collected over the range $5° < 2\theta < 80°$ (step scan: 0.50 s, step width: 0.02° 2θ) at room temperature using an Ital Structure APD2000 X-ray diffractometer with Cu $K\alpha$ radiation (λ = 1.5418 Å). The phase purity of the products after thermal decomposition of the complexes is confirmed by comparison of the XRPD data to the JCPDS cards. Magnetic properties were studied between 2 and 300 K in a magnetic field of H = 1000 Oe and at a constant temperature of 5 K between H = ± 50 kOe with a Quantum Design MPMS-XL-5 SQUID magnetometer. The measured data were corrected for a sample holder contribution and for a temperature independent Larmor diamagnetism of core electrons obtained from Pascal's tables.[22]

2. 2. Synthesis of $[Ni(dipya)_2(H_2O)_2](tpht) \cdot 2H_2O$, (1)

The synthesis of the complex **1** has been an attempt to obtain Ni–tpht complex with two N,N-donor ligands, dipya and 1,10-phenanthroline (phen), in the same structure. Into an aqueous solution of $Ni(NO_3)_2 \cdot 6H_2O$ (0.291 g, 1.00 mmol) in 100 mL of water a mixed solution of dipya (0.171 g, 1.00 mmol) and phen (0.198 g, 1.00 mmol) in 15 mL of EtOH was added. Then, the 50 mL of an aqueous solution of Na_2tpht (0.208 g, 1.00 mmol) was added drop wise at room temperature under continuous magnetic stirring. The final solution was transferred to a crystallization dish and left under ambient conditions for slow evaporation. The violet single crystals of suitable size, insoluble in water, ethanol and DMSO, were obtained after 15 days. Single-crystal XRD analysis confirmed that dipya is the only N,N-donor ligand in the complex **1**. Yield: 42 %; FTIR (cm^{-1}): 3410 (O–H and N–H), 1639 (C=N), 1564 (COO), 1487 (C–C), 1369 (COO), 770 (C–H).

2. 3. Synthesis of $[Co(dipya)_2(H_2O)_2](tpht) \cdot 2H_2O$, (2)

The synthesis of the complex **2** has been an attempt to obtain a heterometallic Mn–Co complex with tpht and dipya ligands. The reaction mixture of 1 M $Mn(NO_3)_2$ (0.1 cm^3, 0.1 mmol), 1 M $Co(NO_3)_2$ (0.1 cm^3, 0.1 mmol), dipya (0.0342 g, 0.2 mmol), 0.2 M Na_2tpht (1.0 cm^3, 0.2 mmol) and H_2O (3 cm^3) was placed in a Teflon-lined steel autoclave, heated for 96 h at 160 °C and cooled for 8 h to room temperature. The orange single crystals, insoluble in water, ethanol and DMSO, were obtained. AAS was confirmed the presence of Co(II) ions only in the obtained crystals. Yield: 38 %; FTIR (cm^{-1}): 3416 (O–H and N–H), 1637 (C=N), 1560 (COO), 1473 (C–C), 1369 (COO), 770 (C–H).

2. 4. X-ray Structure Determination of 1 and 2

Single-crystal X-ray diffraction data for **1** and **2** were collected at room temperature (298 K) on an Oxford Gemini S diffractometer equipped with CCD detector using monochromatized Mo $K\alpha$ radiation (λ = 0.71073 Å). Intensities were corrected for absorption using the multiscan method. Because of the dimensions of the single crystal **1** (Table 1), additional Gaussian correction for absorption was applied. The structures were solved by direct methods using SIR2014[23] and refined on F^2 by full-matrix least-squares using the programs SHELXL-2014/7[24] and WinGX.[25] All non-hydrogen atoms were refined anisotropically. Positions of the H atoms connected to C and N atoms were calculated on geometric criteria and refined using the riding model with $U_{iso} = 1.2U_{eq}$(C, N). In both structures, one water molecule was disordered with congener atoms, O8A and O8B, having about 60 and 40% site occupancies. Water H atoms for O1 and O2 were found in

Δ*F* maps. Water H atoms for O8A and O8B were also found in Δ*F* maps and refined with O–H distances restrained to 0.85 Å. Positions of water H atoms for O7 were calculated using the program HYDROGEN[26] and added to the structural model before the final cycle of refinement with fixed coordinates and with $U_{iso}(H) = 1.5U_{eq}(O)$. For water H34 atom in **1** and H33 atom in **2** were not possible to identify suitable hydrogen bond acceptors. Selected crystal data and refinement results for **1** and **2** are listed in Table 1.

3. Results and Discussion

3. 1. Description of the Crystal Structures

According to the single-crystal X-ray diffraction analysis, complexes **1** and **2** crystallize in the monoclinic *P*2/*c* space group. The solid-state structures consist of individual $[M(dipya)_2(H_2O)_2]^{2+}$ entities, two counter $tpht^{2-}$ ions and two lattice water molecules (Figures 1 and S1). Due to the isostructurality of the structures, only the figures related to **1** will be presented in the manuscript. The geometry around the M(II) center is distorted octahedral with three N atoms (N1, N2 and N5) from two chelate dipya ligands and O1 atom from one water molecule in equatorial plane, while N4 atom from dipya and O2 atom from another water molecule occupy the apical positions. The bond lengths and angles (Table 2) are as expected for dipya–tpht TM complexes with octahedral environment.[11–14] The deviation of M(II) atom from planarity of the equatorial plane is not substantial, being 0.0024(6) Å for **1** and only 0.0011(6) Å for **2**, while the shortest M(II)···M(II) distances are 7.660(2) and 7.664(2) Å in **1** and **2**, respectively. The similar $[M(dipya)_2(H_2O)_2]^{2+}$ cation was also found in compound $[Co(dipya)_2(H_2O)_2]_2[Hdipya][PCoW_{11}O_{39}]$,[27] but with slightly smaller deviation of Co(II) atom from the basal plane of polyhedron (0.009 Å).

Since the crystallographic inversion centers coincide with the centers of both tpht aromatic rings, only a half of each tpht ion belongs to the asymmetric unit. In the packing, the dihedral angle between two tpht aromatic rings amounts 74.3(1)° in **1** and 75.1(1)° in **2**. The deviation from planarity of tpht ligands is noticeable with the angle between C26–C28 ring and adjacent COO group of 25.6(2)° in **1** and 26.0(2)° in **2**, while the analogous angle for C22–C24 ring is 18.6(1)° in both complexes. As it was mentioned in the introduction, in TM–tpht complexes (containing at least one tpht as a counter anion) with different N,N-donor ligands,[16–21] these angles were found to be in the range between 17.4 and 29.0°.

Table 1. Crystal data and structure refinements for **1** and **2**.

Complex	**1**	**2**
Formula	$C_{28}H_{30}N_6O_8Ni$	$C_{28}H_{30}N_6O_8Co$
Formula weight (g mol^{-1})	637.29	637.51
Crystal size (mm^3)	0.62 × 0.44 × 0.40	0.24 × 0.24 × 0.12
Crystal system	Monoclinic	Monoclinic
Space group	*P*2/*c*	*P*2/*c*
a (Å)	9.705(2)	9.746(2)
b (Å)	9.795(2)	9.797(2)
c (Å)	30.303(6)	30.287(6)
α (°)	90	90
β (°)	97.43(3)	97.40(3)
γ (°)	90	90
V (Å^3)	2856.5(10)	2867.9(10)
Z	4	4
F(000)	1328	1324
μ (mm^{-1})	0.741	0.659
ρ_c (g cm^{-3})	1.482	1.477
Reflections collected/unique	17377/5603	29474/5630
R_{int}	0.0268	0.0234
Data/restraints/parameters	4892/4/420	5260/4/420
R indices [$I > 2\sigma(I)$]	$R = 0.0395$, $R_w = 0.0882^{\dagger}$	$R = 0.0354$, $R_w = 0.0833^{\ddagger}$
R indices (all data)	$R = 0.0478$, $R_w = 0.0920$	$R = 0.0388$, $R_w = 0.0851$
Goodness-of-fit	1.121	1.152
$\Delta\rho_{max}$, $\Delta\rho_{min}$ (e Å^{-3})	0.529, –0.382	0.318, –0.391

$^{\dagger}w = 1 / [s^2 \cdot (F_o^2) + (0.0341 \cdot P)^2 + 1.9123 \cdot P]$ where $P = (F_o^2 + 2 \cdot F_c^2) / 3$ $^{\ddagger}w = 1 / [s^2 \cdot (F_o^2) + (0.0337 \cdot P)^2 + 1.6366 \cdot P]$ where $P = (F_o^2 + 2 \cdot F_c^2) / 3$

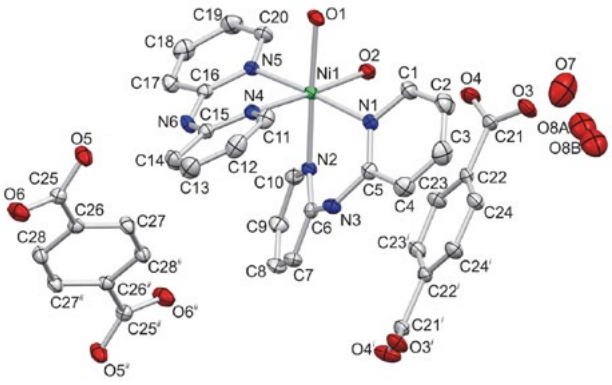

Figure 1. Structural fragment of **1** with atomic numbering scheme (hydrogen atoms are omitted for the sake of clarity). The thermal ellipsoids are plotted at the 30% probability level. Symmetry codes: *(i)* $-x+1, y, -z+½$, *(ii)* $-x+1, -y+2, -z$.

The stabilization of the crystal lattices of **1** and **2** is achieved by the hydrogen bonds and non-covalent interactions. The hydrogen bond network (Table 3) includes all water molecules, all COO^- groups and both dipya ligands as it is shown in Figures 2 and S2. The analysis of the crystal packing in **1** and **2** manifested the difference in the position of the O7 water molecule that is in **2** shifted to the symmetry equivalent position relative to its position in **1**. The network of hydrogen bonds permit the formation of three supramolecular chains along [100], [010] and [001] directions and thus forming 3D network. The centroid *Cg*···*Cg* distances found between C6–C10/N2 pyridyl ring of dipya and C22–C24 aromatic ring are 3.904(2) and 3.899(1) Å in **1** and **2**, respectively. These distances indicate weak face to face π-π interactions (Figures 3 and S3).[28] Furthermore, several C–H···O and one C–H···N interactions, which geometries are presented in Table S1, form short contact clusters allowing additional networking in both structures.

Table 2. Selected bond lengths and angles for **1** and **2**.

Bond lengths, Å		Angles, °	
1			
Ni1–N1	2.086(2)	N1–Ni1–N2	84.42(8)
Ni1–N2	2.098(2)	N1–Ni1–N4	93.88(7)
Ni1–N4	2.090(2)	N1–Ni1–N5	176.1(1)
Ni1–N5	2.097(2)	N1–Ni1–O1	94.01(8)
NI1–O1	2.084(2)	N1–Ni1–O2	89.17(8)
NI1–O2	2.070(2)	N2–Ni1–N4	90.23(7)
		N2–Ni1–N5	91.66(7)
		N2–Ni1–O1	178.2(1)
		N2–Ni1–O2	90.68(8)
		N4–Ni1–N5	86.19(7)
		N4–Ni1–O1	90.78(8)
		N4–Ni1–O2	176.9(1)
		N5–Ni1–O1	89.90(7)
		N5–Ni1–O2	90.82(8)
		O1–Ni1–O2	88.39(8)
2			
Co1–N1	2.131(2)	N1–Co1–N2	82.47(6)
Co1–N2	2.152(2)	N1–Co1–N4	94.58(6)
Co1–N4	2.142(2)	N1–Co1–N5	174.1(1)
Co1–N5	2.140(2)	N1–Co1–O1	93.48(7)
Co1–O1	2.091(2)	N1–Co1–O2	89.51(6)
Co1–O2	2.097(2)	N2–Co1–N4	88.93(6)
		N2–Co1–N5	91.64(6)
		N2–Co1–O1	176.0(1)
		N2–Co1–O2	91.41(6)
		N4–Co1–N5	84.92(6)
		N4–Co1–O1	91.44(7)
		N4–Co1–O2	175.9(1)
		N5–Co1–O1	92.41(6)
		N5–Co1–O2	90.98(6)
		O1–Co1–O2	88.50(7)

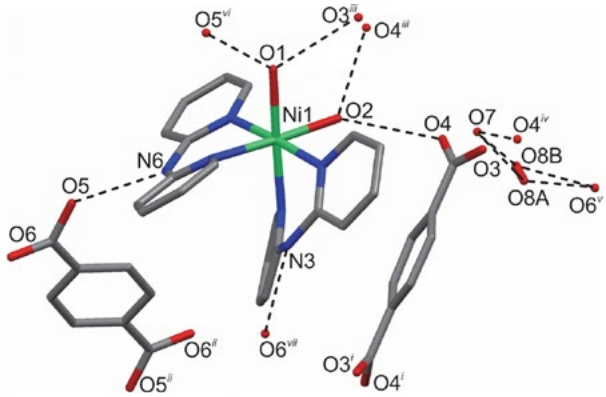

Figure 2. The network of hydrogen bonds (presented by dashed lines) in **1**. Hydrogen atoms are omitted for the sake of clarity.

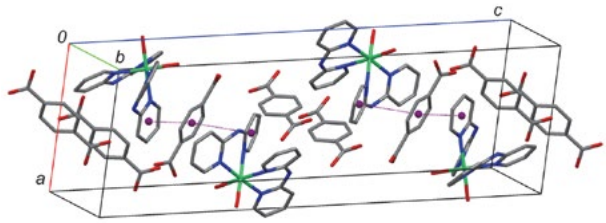

Figure 3. Projection of the crystal packing of **1** in almost *ac*-plane. The π-π interactions between structural fragments are presented by purple lines.

3. 2. Thermal Properties

The dehydration of **1** is an endothermic process occurring in a single step up to 153 °C with a loss of four water molecules (found 11.4%, calc. 11.3%) (Figure 4). The determined enthalpy of dehydration obtained by integration of DSC peak area is 218 kJ mol^{-1}, and it is in a good agreement with values that were already found for several similar ternary BDC complexes.[11,29,30] It was previously evaluated that average molar enthalpy per one hydrogen

Table 3. The geometry of hydrogen bonds for **1** and **2**.

D–H···*A*	*d*(*D*–H), Å	*d*(*D*···*A*), Å	*d*(H···*A*), Å	*D*–H···*A*, °
1				
O1–H30···O3^{iii}	0.858(5)	2.729(3)	1.874(5)	174(3)
O1–H29···O5^{vi}	0.801(3)	2.848(3)	2.054(3)	171(3)
O2–H32···O4	0.739(7)	2.998(3)	2.361(9)	145(4)
O2–H31···O4^{iii}	0.816(8)	2.617(3)	1.803(8)	176(4)
O7–H33···O4^{iv}	0.870(9)	2.830(4)	2.004(1)	158(5)
O8A–H36···O6^{v}	0.830(1)	2.870(1)	2.139(2)	147(3)
O8B–H36···O6^{v}	0.855(8)	2.978(7)	2.139(2)	167(3)
O8A–H35···O7	0.891(6)	2.887(2)	2.025(5)	162(3)
O8B–H35···O7	0.817(1)	2.775(6)	2.025(5)	153(4)
N3–H3A···O6^{vii}	0.86	2.887(3)	2.09	154
N6–H6···O5	0.86	2.809(3)	2.04	149
2				
O1–H30···O3^{iii}	0.812(2)	2.717(3)	1.909(2)	174(3)
O1–H29···O5^{vi}	0.806(6)	2.824(2)	2.019(5)	176(3)
O2–H32···O4	0.734(1)	2.968(2)	2.305(2)	151(3)
O2–H31···O4^{iii}	0.835(4)	2.610(2)	1.776(4)	175(3)
O7–H34···O4	0.828(1)	2.828(3)	2.034(1)	161(4)
O8A–H35···O6^{v}	0.814(6)	2.864(8)	2.137(7)	149(2)
O8B–H35···O6^{v}	0.853(1)	2.966(2)	2.137(7)	164(3)
O8A–H36···O7^{iv}	0.901(9)	2.875(9)	2.023(9)	157(3)
O8B–H36···O7^{iv}	0.804(2)	2.779(2)	2.023(9)	157(3)
N3–H3A···O6^{vii}	0.86	2.884(2)	2.09	153
N6–H6···O5	0.86	2.810(2)	2.02	152

Symmetry codes: **1** (*iii*) $-x, y, -z + ½$; (*iv*) $x, y - 1, z$; (*v*) $x, -y + 1, z + ½$; (*vi*) $-x, -y + 1, -z$; (*vii*) $-x + 1, -y + 1, -z$; **2** (*iii*) $-x, y, -z + ½$; (*iv*) $x, y - 1, z$; (*v*) $x, -y + 1, z + ½$; (*vi*) $-x, -y + 1, -z$; (*vii*) $-x + 1, -y + 1, -z$.

bond is about 16 kJ mol^{-1}.[30] In **1**, four water molecules participate in the formation of even nine hydrogen bonds, thus it can be conclude that molar enthalpy per one Ni–OH_2 coordinative bond is equal to 37 kJ mol^{-1}. Further degradation of complex happens in two temperature ranges, 153–336 °C and 336–1100 °C, with a loss of complete tpht anion (found 36.1%, calc. 37.1%) and two dipya molecules (found 90.3%, calc. 90.8%), respectively. The final residual mass 9.68% (calc. 9.21%) is in good agreement with the formation of pure Ni as a decomposition product, whose identity was verified by XRPD (Figure S4). In inert atmosphere, the decomposition of TM complexes to pure metal is not unusual as it was proven in previous studies.[31,32] The thermal behavior of **2** follows a very similar pattern, giving metallic Co as a final product (found 9.88%, calc. 9.24%, Figure S5). Both products obtained after decomposition of the complexes at 1100 °C were analyzed using XRPD (Figures S4 and S6) and the presence of Ni and Co for **1** and **2**, respectively, was confirmed by comparing the XRPD patterns with standard cards.

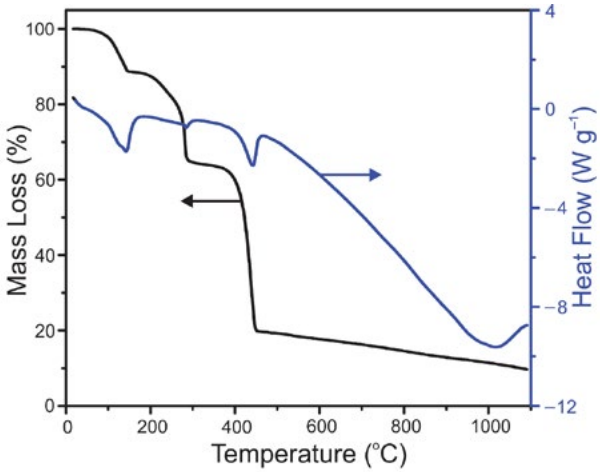

Figure 4. TGA and DSC curves for **1** obtained at heating rate of 10 °C min^{-1} in flowing N_2 (exo up).

3. 3. Magnetic Properties

Temperature dependent susceptibility of **1** measured in a magnetic field of $H = 1000$ Oe is shown in Figure 5a. It follows a Curie-like $1/T$ dependence. Only a small deviation from a perfect paramagnetic behavior can be seen as a

small decrease of the product χT below 10 K in otherwise temperature constant product χT (inset in Figure 5a). The value of χT between 20 and 300 K is 1.2 emu K mol^{-1}, which falls in the expected range for uncoupled Ni(II) ion.[33] The magnetization curve of **1** at 5 K is presented in Figure 5b. The measured data can be excellently described with a Brillouin function (full green line) for spin $S = 1$ as expected for Ni(II).

Taking into account the constant χT for $T > 20$ K and paramagnetic behavior of isothermal magnetization, we ascribe the weak temperature variation of the product χT below 10 K to a zero-field splitting of Ni(II) ion with d^8 configuration in a distorted octahedral environment. The average susceptibility for polycrystalline sample $\chi = (\chi_z + 2\chi_x) / 3$ and $g_z = g_x = g$ can be written as[22]

$$\chi = \frac{2N_A g^2 \mu_B^2}{3k_B T} \frac{(2k_B T / D)\left[1 - \exp(D / k_B T)\right] + \exp(D / k_B T)}{1 + 2\exp(-D / k_B T)} \quad (1)$$

where N_A is Avogadro number, μ_B is Bohr magneton and D is zero-field splitting parameter. The result of fitting procedure (full line in inset in Figure 5a) are parameters $g = 2.19$ and $D = 3.6$ cm^{-1} with $\overline{R^2} > 0.96$. The zero-field splitting parameter D is of the same order as determined in our previous work.[29]

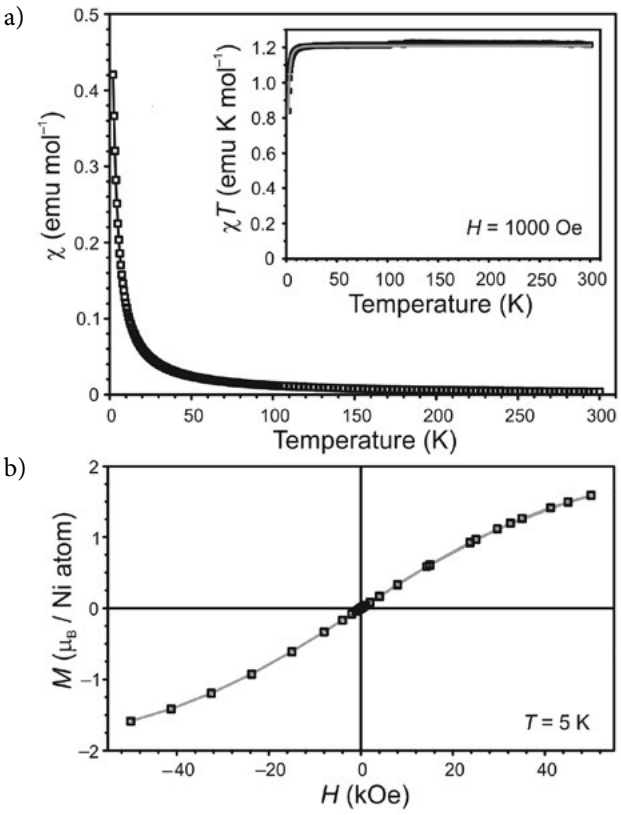

Figure 5. Temperature variation of magnetic susceptibility measured in $H = 1000$ Oe of **1** and the product χT. The green line is a fit with function (1) (a). Isothermal magnetization at 5 K and a Brillouin function (green line) for spin $J = 1$ of **1** (b).

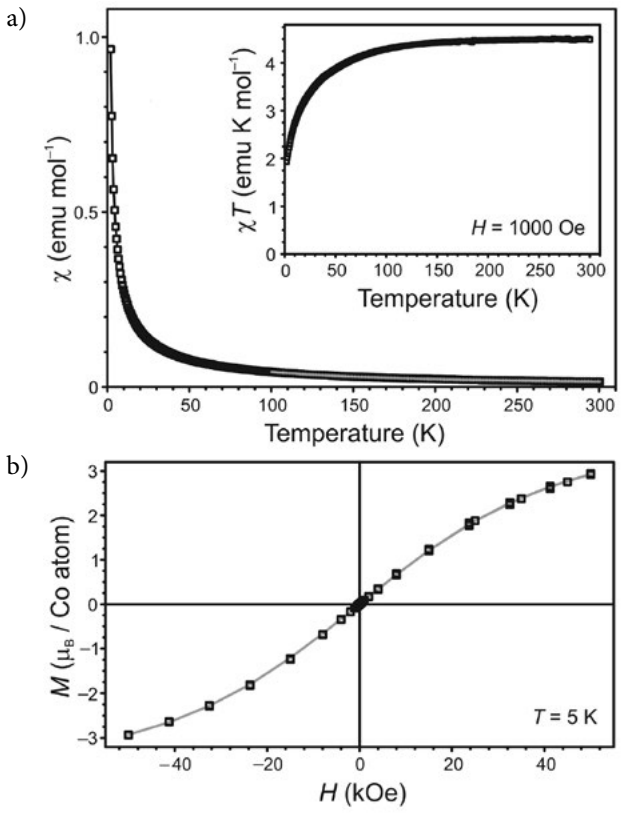

Figure 6. Temperature variation of magnetic susceptibility and the product χT (inset) measured in $H = 1000$ Oe of **2**. The green line is a fit with the Curie-Weiss function (a). Isothermal magnetization at 5 K and a Brillouin function (green line) for spin $J = 3/2$ of **2** (b).

Figure 6a shows the susceptibility for **2** in a temperature range from 2 to 300 K. The Curie-Weiss fit $\chi = C / (T - \theta)$ was performed on the data for $T > 100$ K. The obtained Curie constant, $C = 4.6$ emu K mol^{-1}, is in the range for Co(II) ions with a total electronic spin angular momentum $S = 3/2$ and a non-zero contribution of total orbital angular moment L.[33] The negative Curie-Weiss temperature $\theta = -7.9$ K is in agreement with the reduction of the product χT (inset in Figure 6a) with decreasing temperature. The negative θ can be an indication of a weak antiferromagnetic interaction between magnetic moments or the result of a single ion effects (L-S coupling of Co(II) ions[34] in distorted octahedral environment and zero-field splitting). As the isothermal magnetization (Figure 6b) perfectly follows the Brillouin function for isolated ions with no indication of antiferromagnetic interaction, we contribute the negative θ and reduction of the product χT with decreasing temperature to the combined effect of L-S coupling and zero-field splitting of non-interacting Co(II) ions.

4. Conclusion

Two discrete, isostructural complexes, [M(dipya)$_2$(H$_2$O)$_2$](tpht) · 2H$_2$O (M = Ni, Co), have been synthesized

by ligand exchange reaction. The compounds are structurally characterized and their spectral, thermal and magnetic properties were determined. Single crystal X-ray analysis revealed that the geometry around M(II) ions is deformed octahedral, while the supramolecular packing is achieved by the combination of hydrogen bonds, π-π, C–H···O and C–H···N interactions. Thermal decomposition of both complexes up to 1100 °C yielded pure metals. The temperature dependent magnetic susceptibility data indicated that there were not magnetic interaction between M(II) ions. The contribution of the *L-S* coupling is observed with parameters g and D of 2.19 and 3.6 cm^{-1}, respectively, for **1** and θ of –7.9 K for **2**.

5. Acknowledgements

This work was supported financially by the Ministry of Education, Science and Technological Development of the Republic of Serbia (Grant No. III45007) and from Slovenian Research Agency (Grant No. P2-0348).

6. Appendix A. Supplementary Materials

CCDC 1539377 and 1539378 contain the supplementary crystallographic data for compounds **1** and **2**. These data can be obtained free of charge from the Cambridge Crystallographic Data Centre via www.ccdc.cam.ac.uk/data_request/cif. Supplementary data associated with this article can be found, in the online version.

7. References

1. T. R. Cook, Y. R. Zheng, P. J. Stang, *Chem. Rev.* **2013**, *113*, 734–777. **DOI:**10.1021/cr3002824
2. Z. H. Li, W. J. Ao, X. X. Wang, X. Z. Fu, *Acta Crystallogr.* **2006**, *E62*, m1048–m1050. **DOI:**10.1107/S1600536806012748
3. C. B. Ma, M. Q. Hu, C. X. Zhang, F. Chen, C. N. Chen, Q. T. Liu, *Acta Crystallogr.* **2004**, *C60*, m288–m290. **DOI:**10.1107/S0108270104007565
4. G. H. Wang, Z. G. Li, H. Q. Jia, N. H. Hu, J. W. Xu, *Cryst. Growth Des.* **2008**, *8*, 1932–1939. **DOI:**10.1021/cg701232n
5. B. P. Yang, H. Y. Zeng, J. G. Mao, G. C. Guo, J. S. Huang, *Transit. Met. Chem.* **2003**, *28*, 600–605. **DOI:**10.1023/A:1025096207371
6. E. G. Bakalbassis, J. Mrozinski, C. A. Tsipis, *Inorg. Chem.* **1985**, *24*, 3548–3553. **DOI:**10.1021/ic00216a015
7. C. Janiak, *Dalton Trans.* **2003**, 2781–2804. **DOI:**10.1039/b305705b
8. C. S. Hong, Y. S. You, *Polyhedron* **2004**, *23*, 3043–3050. **DOI:**10.1016/j.poly.2004.09.019
9. H. X. Zhang, B. S. Kang, A. W. Xu, Z. N. Chen, Z. Y. Zhou, A. S. C. Chan, K. B. Yu, C. Ren, *J. Chem. Soc., Dalton Trans.* **2001**, 2559–2566. **DOI:**10.1039/b102570h
10. C. R. Groom, I. J. Bruno, M. P. Lightfoot, S. C. Ward, *Acta Crystallogr.* **2016**, *B72*, 171–179. **DOI:**10.1107/S2052520616003954
11. L. Radovanović, J. Rogan, D. Poleti, M. V. Rodić, N. Begović, *Inorg. Chim. Acta* **2016**, *445*, 46–56. **DOI:**10.1016/j.ica.2016.02.026
12. J. Rogan, D. Poleti, Lj. Karanović, G. A. Bogdanović, A. Spasojević-de Biré, D. M. Petrović, *Polyhedron* **2000**, *19*, 1415–1421. **DOI:**10.1016/S0277-5387(00)00435-6
13. E. Yang, Y. Zheng, G. Y. Chen, *Acta Crystallogr.* **2006**, *E62*, m1079–m1080. **DOI:**10.1107/S1600536806013717
14. Lj. Karanović, D. Poleti, J. Rogan, G. A. Bogdanović, A. Spasojević-de Biré, *Acta Crystallogr.* **2002**, *C58*, m275–m279. **DOI:**10.1107/S0108270102004341
15. L. Radovanović, J. Rogan, D. Poleti, M. Milutinović, M. V. Rodić, *Polyhedron* **2016**, *112*, 18–26. **DOI:**10.1016/j.poly.2016.03.054
16. H. Xu, Y. Liang, Z. Su, Y. Zhao, K. Shao, H. Zhang, S. Yue, *Acta Crystallogr.* **2004**, *E60*, m142–m144. **DOI:**10.1107/S1600536803029210
17. W. Huang, D. Hu, S. Gou, H. Qian, H. K. Fun, S. S. S. Raj, Q. Meng, *J. Mol. Struct.* **2003**, *649*, 269–278. **DOI:**10.1016/S0022-2860(03)00080-2
18. H. P. Xiao, Z. Shi, L. G. Zhu, R. R. Xu, W. Q. Pang, *Acta Crystallogr.* **2003**, *C59*, m82–m83. **DOI:**10.1107/S0108270103002087
19. X. Li, D. Cheng, J. Lin, Z. Li, Y. Zheng, *Cryst. Growth. Des.* **2008**, *8*, 2853–2861. **DOI:**10.1021/cg701150q
20. H. M. Zhang, L. P. Lu, S. S. Feng, S. D. Qin, M. L. Zhu, *Acta Crystallogr.* **2005**, *E61*, m1027–m1029. **DOI:**10.1107/S160053680501322X
21. R. P. Sharma, A. Singh, P. Venugopalan, W. T. A. Harrison, *J. Mol. Struct.* **2010**, *980*, 72–77. **DOI:**10.1016/j.molstruc.2010.06.039
22. O. Kahn, in: Molecular Magnetism, VCH Publishing, **1993**.
23. M. C. Burla, R. Caliandro, B. Carrozzini, G. L. Cascarano, C. Giacovazzo, M. Mallamo, A. Mazzone, G. Polidori, *J. Appl. Crystallogr.* **2015**, *48*, 306–309. **DOI:**10.1107/S1600576715001132
24. G. M. Sheldrick, *Acta Crystallogr.* **2015**, *C71*, 3–8. **DOI:**10.1107/S2053229614024218
25. L. J. Farrugia, *J. Appl. Crystallogr.* **2012**, *45*, 849–854. **DOI:**10.1107/S0021889812029111
26. M. Nardelli, *J. Appl. Crystallogr.* **1999**, *32*, 563–571. **DOI:**10.1107/S0021889899002666
27. B. Yan, Y. Xu, X. Bu, N. K. Goh, L. S. Chia, G. D. Stucky, *J. Chem. Soc., Dalton Trans.* **2001**, 2009–2014. **DOI:**10.1039/b103024h
28. C. Janiak, *J. Chem. Soc., Dalton Trans.* **2000**, 3885–3896. **DOI:**10.1039/b003010o
29. J. Rogan, D. Poleti, Lj. Karanović, Z. Jagličić, *J. Mol. Struct.* **2011**, *985*, 371–379. **DOI:**10.1016/j.molstruc.2010.11.024
30. J. Rogan, D. Poleti, *Thermochim. Acta* **2004**, *413*, 227–234. **DOI:**10.1016/j.tca.2003.10.015

31. N. Parveen, R. Nazir, M. Mazhar, *J. Therm. Anal. Calorim.* **2013**, *111*, 93–99.
DOI:10.1007/s10973-011-2185-2
32. C. Hopa, R. Kurtaran, M. Alkan, H. Kara, R. Hughes, *Transit. Met. Chem.* **2010**, *35*, 1013–1018.
DOI:10.1007/s11243-010-9424-4
33. N. W. Ashcroft, N. D. Mermin, in: Solid State Physics, Saunders College Publishing, USA, **1976**.
34. F. Lloret, M. Julve, J. Cano, R. Ruiz-García, E. Pardo, *Inorg. Chim. Acta* **2008**, *361*, 3432–3445.
DOI:10.1016/j.ica.2008.03.114

Povzetek

Z reakcijo izmenjave ligandov smo sintetizirali dva nova izostrukturna M(II) (M = Ni, Co) kompleksa z 2,2'-dipiridilaminom (dipya) in dianionom tereftaline kisline (H_2tpht), [M(dipya)$_2$(H_2O)$_2$](tpht) · 2H_2O, in ju okarakterizirali z monokristalno rentgensko difrakcijo, FTIR spektroskopijo, TG/DSC analizo in magnetnimi meritvami. Kristalni strukturi [M(dipya)$_2$(H_2O)$_2$](tpht) · 2H_2O sta zgrajeni iz izoliranih kompleksnih enot, v katerih ima M(II) ion popačeno oktaedrično geometrijo. Dva dipya liganda in dve molekuli vode so koordinirani na M(II) ion, tpht je protiion, preostali dve molekuli vode sta v strukturi nekoordinirani. Strukturni fragmenti so povezani preko številnih vodikovih vezi v tri verige vzdolž [100], [010] in [001] smeri, kar vodi do nastanka 3D mreže. Stabilizacija 3D strukture je dosežena z nekovalentnimi π-π interakcijami med piridinskimi obroči dipya ligandov in benzenovih obročev tpht anionov iz sosednjih verig. V magnetnem polju izkazujeta oba kompleksa popolno paramagnetno obnašanje.